FRACTAL CONICAL SECTIONS AND ORBITS: QUALITATIVE FAILURE OF THE EINSTEINIAN GENERAL RELATIVITY.

by

M. W. Evans, H. Eckardt, R. Delaforce and G. J. Evans

Civil List and A.I.A.S

(www.aias.us, www.atomicprecision.com, www.upitec.org, www.et3m.net, www.webarchive.org.uk)

ABSTRACT

The conical sections are shown to develop fractal properties when modified with the precession factor x. In theory these are observable orbits. Use of the equation of the fractal orbits shows that the Einsteinian general relativity (EGR) fails qualitatively in several, easily demonstrated, ways, notably, EGR never develops into fractal orbits, and its orbit equation is incorrect qualitatively when compared with the correct fractal orbit equation. All fractal orbits are governed by the same universal law of gravitation on the classical level. The universal gravitational potential has the same format as the potential of the Schroedinger equation so in theory there exists a gravitational Schroedinger equation and fractal orbits of electrons can be deduced from electron orbitals in atoms and molecules.

Keywords: Classical limit of ECE theory, fractal conical sections and orbits, qualitative failure of the Einsteinian general relativity.

1. INTRODUCTION

It is well known that the precessing ellipse represents a large class of orbits from the solar system to binary neutron stars. The ellipse is a conical section with eccentricity less than one, and is the orbit in a plane of Newtonian dynamics. Recently in this series of papers {1 - 10} it has been shown that the precession of the ellipse can be represented by a dimensionless precession factor x that multiplies the polar angle θ in the equation of the ellipse and the conical sections in general. All precessing elliptical orbits can be described by the parameter x on the classical level. In recent papers, lagrangian dynamics have been used in the classical limit of ECE theory {1 - 10} to show that the precessing elliptical orbits are governed by a universal law of gravitation on the classical level. In Section 2 it is shown straightforwardly that the Einsteinian general relativity (EGR) fails qualitatively to produce a precessing ellipse and is therefore an irretrievably incorrect theory at the basic level. The largest value of x observed in cosmology seems to be that of a binary neutron star system PSR J0737-3039, in which x is 1.0469. In the Hulse Taylor binary pulsar x is 1.0117, and in the solar system $x - 1$ is of the order 10^{-8}. However, in mathematics, x can take any value and when it is increased or decreased from unity (the Newtonian value of x), new and hitherto unknown conical sections appear of an infinite variety. These contain repeated patterns and are therefore fractal conical sections. For several hundred years the conical sections have been identified with orbits and the first identification was made by Kepler for the elliptical orbit of Mars. Later it was discovered that the elliptical orbit precesses. Therefore in theory, the fractal conical sections produce hitherto undiscovered orbits of infinite variety, all governed by the same universal gravitational potential on the classical level, completely without EGR. The universal gravitational potential has the same mathematical structure precisely as the effective potential of the Schroedinger equation, so

this type of potential applies from super galactic to electronic scales. So in theory there exists a gravitational Schroedinger equation and fractal electron orbits from electronic orbitals. These are discussed briefly in Section 2 with reference to the background notes for UFT217 on www.aias.us.

In Section 3 the fractal properties of the x modified conical sections are illustrated graphically. The qualitative (i.e. total) failure of EGR is illustrated with the orbit equation and with the equation for orbit linear velocity. The structure of EGR is such that it cannot produce the fractal orbits, so EGR was a false turn in cosmology. The 1788 methods of Lagrange have turned out to give an infinite variety of orbits all observable in theory.

2. FRACTAL CONICAL SECTIONS AND ORBITS

The equation of the conical sections modified by x is:

$$r = \frac{\alpha}{1 + \epsilon \cos(x\theta)} \qquad -(1)$$

where (r, θ) is the cylindrical plane polar system of coordinates. Here α is the half right latitude, ϵ is the eccentricity and x the precession or fractal factor. By differentiation:

$$\frac{dr}{d\theta} = \frac{x\epsilon}{\alpha} r^2 \sin(x\theta) \qquad -(2)$$

and this is the equation of orbits. In Eq. (1):

$$\alpha = \frac{L^2}{mk}, \quad \epsilon = \left(1 + \frac{2EL^2}{mk^2}\right)^{1/2}, \quad k = mMG, \qquad -(3)$$

where E and L are two constants of motion, the total energy and total angular momentum respectively, both being conserved quantities. The constant k is defined by:

$$k = mMG \qquad -(4)$$

where the mass m orbits the mass M in a plane, and where G is Newton's constant:

$$G = 6.67265 \times 10^{-11}\ m^3 s^{-2} kg^{-1} \quad -(5)$$

EGR claims that {11,12}:

$$\frac{dr}{d\theta} = r^2 \left(\frac{1}{b^2} - \left(1 - \frac{r_0}{r}\right)\left(\frac{1}{a^2} + \frac{1}{r^2}\right)\right)^{1/2} \quad -(6)$$

where the constants a, b and r_0 are defined by:

$$a = \frac{L}{mc}, \quad b = \frac{Lc}{E}, \quad r_0 = \frac{2MG}{c^2}, \quad -(7)$$

where c is the claimed constant speed of light in vacuo. In Section 3 it is shown that eq. (2) and (6) give qualitatively different results. Graphical methods show that Eq. (1) for x close to unity is a precessing ellipse, so Eq. (6) does not give a precessing ellipse QED. Therefore EGR fails at a basic level, and claims based on EGR are meaningless in science.

The orbital linear velocity is given by {1 - 10}:

$$v^2 = \left(\frac{dr}{dt}\right)^2 + r^2 \left(\frac{d\theta}{dt}\right)^2 \quad -(8)$$

Using:

$$\frac{dr}{dt} = \frac{dr}{d\theta}\frac{d\theta}{dt} \quad -(9)$$

it is found that:

$$v^2 = \left(\frac{d\theta}{dt}\right)^2 \left(\left(\frac{dr}{d\theta}\right)^2 + r^2\right) \quad -(10)$$

and from Eq. (1):

$$v^2 = r^2\left(\frac{d\theta}{dt}\right)^2\left(1 + \left(\frac{r\chi\epsilon}{d}\sin(\chi\theta)\right)^2\right). \quad -(11)$$

The angular velocity is given by {1 - 10}:

$$\frac{d\theta}{dt} = \frac{L}{mr^2} \quad -(12)$$

so the orbital linear velocity is:

$$v = \frac{L}{mr}\left(1 + \left(\frac{r\chi\epsilon}{d}\sin(\chi\theta)\right)^2\right)^{1/2}. \quad -(13)$$

EGR claims that {1 - 11, 12}:

$$v = \frac{cb}{r}\left(1 - \frac{r_0}{r}\right)\left(r^2\left(\frac{1}{b^2} - \left(1 - \frac{r_0}{r}\right)\left(\frac{1}{a^2} + \frac{1}{r^2}\right) + 1\right)\right)^{1/2}. \quad -(14)$$

In Section (3) it is shown graphically that Eq. (14) is again qualitatively different from Eq. (13), which is obtained from the observed precessing ellipse. So EGR has been shown in a second way to be basically incorrect, QED.

It has been shown in previous work {1 - 11} using straightforward Lagrangian methods that the fractal orbit (1) is given for all x by the universal gravitational potential:

$$U(r) = -\frac{k\chi^2}{r} + (\chi^2 - 1)\frac{kd}{2r^2}. \quad -(15)$$

This is a sum of terms inverse in r and inverse squared in r. EGR on the other hand gives a potential {11, 12} that is a sum of terms inverse in r and inverse cubed in r. Therefore EGR does not give the precessing ellipse (1) for x close to unity, QED. It has been shown in a third way that EGR is incorrect at a basic level. The demonstration is straightforward and irrefutable. It follows that EGR never gives fractal orbits based on the fractal conical sections.

The universal potential (15) is obtained straightforwardly from the well known classical Lagrangian equation{1 - 10}

$$\frac{d^2}{d\theta^2}\left(\frac{1}{r}\right) + \frac{1}{r} = -\frac{mr^2}{L} F(r) \quad -(16)$$

where the force F is defined by:

$$F(r) = -\frac{\partial U(r)}{\partial r} . \quad -(17)$$

Using Eq. (1) in the format:

$$\frac{1}{r} = \frac{1}{\alpha}\left(1 + \epsilon \cos(x\theta)\right) \quad -(18)$$

produces the force:

$$F(r) = -\frac{kx^2}{r^2} + (x^2 - 1)\frac{k\alpha}{r^3} \quad -(19)$$

and the potential (15), QED. The Lagrangian is:

$$\mathcal{L} = T - U \quad -(20)$$

where the kinetic energy is:

$$T = \frac{1}{2} m \dot{r}^2 + \frac{L^2}{2mr^2} \quad -(21)$$

and the hamiltonian is the total energy E:

$$H = E = T + U . \quad -(22)$$

The total energy can be expressed as:

$$E = \frac{1}{2} m \dot{r}^2 + \frac{L_1^2}{2mr^2} - \frac{k_1}{r} \quad -(23)$$

where:

$$k_1 = x^2 k, \quad -(24)$$

$$L_1^2 = L^2 - mk\alpha(1 - x^2). \quad -(25)$$

The mathematical format of Eq. (23) is the same as the Newtonian result:

$$E_N = \frac{1}{2} m \dot{r}^2 + \frac{L^2}{2mr^2} - \frac{k}{r}. \quad -(26)$$

In the Newtonian theory use is made of:

$$\frac{d\theta}{dr} = \frac{dr}{dt}\frac{dt}{d\theta}, \quad -(27)$$

$$\frac{d\theta}{dt} = \frac{L}{mr^2}, \quad -(28)$$

$$\frac{dr}{dt} = \left(\frac{2}{r}(E - U) - \frac{L^2}{m^2 r^2}\right)^{1/2}, \quad -(29)$$

$$U = -k/r, \quad -(30)$$

to produce:

$$\theta(r) = \int \frac{L}{m^2}\left(2m\left(E + \frac{k}{r} - \frac{L^2}{2mr^2}\right)\right)^{-1/2} dr \quad -(31)$$

which can be integrated {13, 14} to give the ellipse:

$$r = \frac{\alpha}{1 + \epsilon \cos\theta} \quad -(32)$$

where

$$x = 1. \quad -(33)$$

When x is not unity:

$$L \to L_1, \quad k \to k_1 \qquad -(34)$$

and from eq. (23):

$$\theta_1 = \int \frac{x L_1}{r^2} \left(2m \left(E + \frac{k_1}{r} - \frac{L_1^2}{2mr^2} \right) \right)^{-1/2} dr \qquad -(35)$$

This equation can be integrated to give the result:

$$r = \frac{\alpha_1}{1 + \epsilon_1 \cos\theta_1} \qquad -(36)$$

However, it is known that this result comes from Eqs. (16) and (18), so

$$\theta_1 = x\theta \qquad -(37)$$

In Eq. (18):

$$\alpha \to \alpha_1, \qquad -(38)$$

$$\epsilon \to \epsilon_1, \qquad -(39)$$

so:

$$\alpha_1 = \frac{L_1^2}{mk_1}, \quad \epsilon_1 = \left(1 + \frac{2EL_1^2}{mk_1^2} \right)^{1/2} \qquad -(40)$$

where:

$$L_1^2 = L^2 - mk\alpha(1 - x^2) \qquad -(41)$$

$$= x^2 L^2 .$$

Therefore it is found that:

$$\alpha_1 = \alpha, \qquad -(42)$$

$$\epsilon_1 = \epsilon, \qquad -(43)$$

and that:

$$r = \frac{d}{1 + \epsilon \cos(x\theta)} \quad -(44)$$

is given self consistently from Eq. (15), QED.

The fundamentally new fractal properties of Eq. (44) can be demonstrated as follows. The fractal ellipse is defined by:

$$d = a(1 - \epsilon^2), \quad \epsilon < 1, \quad -(45)$$

where a is the semi major axis. Consider the Cartesian representation of Eq. (44):

$$\frac{(X + a\epsilon)^2}{a^2} + \frac{Y^2}{b^2} = 1 \quad -(46)$$

where:

$$X = a\epsilon + r\cos(x\theta), \quad -(47)$$

$$Y = r\sin\theta, \quad -(48)$$

$$r = a - \epsilon X, \quad -(49)$$

$$\epsilon = \left(1 - \frac{b^2}{a^2}\right)^{1/2}, \quad -(50)$$

and b is the semi minor axis. Then X and Y can be expressed in terms of θ as follows:

$$X = a\epsilon + \frac{d\cos(x\theta)}{1 + \epsilon\cos(x\theta)}, \quad -(51)$$

$$Y = \frac{d\sin(x\theta)}{1 + \epsilon\cos(x\theta)}. \quad -(52)$$

It is shown in Section 3 that these equations give fractal patterns, patterns that are repeated as x is increased. This appears to be a major discovery in pure mathematics, and also in orbital theory, because all known orbits can be described by Eq. (44), including those of galaxies.

It is well known that EGR fails qualitatively in a fourth way because it does not describe

galactic orbits at all.

The fractal hyperbola is described by Eq. (44) with:

$$d = a(\epsilon^2 - 1), \quad \epsilon > 1. \quad -(53)$$

Its Cartesian representation is:

$$\frac{(X - a\epsilon)^2}{a^2} - \frac{Y^2}{b^2} = 1 \quad -(54)$$

where:

$$X = -a\epsilon + r\cos\theta, \quad Y = r\sin\theta, \quad -(55)$$

$$r = -a - \epsilon X, \quad \epsilon = \left(1 + \frac{b^2}{a^2}\right)^{1/2}. \quad -(56)$$

So the X and Y components can be described in terms of θ as follows

$$X = -a\epsilon + \frac{d\cos(x\theta)}{1 + \epsilon\cos(x\theta)}, \quad -(57)$$

$$Y = \frac{d\sin(x\theta)}{1 + \epsilon\cos(x\theta)}, \quad -(58)$$

and again these produce fractal patterns as graphed in Section 3. The fractal parabola is defined by

$$\epsilon = 1 \quad -(59)$$

and again produces hitherto unknown fractal patterns.

Continuing systematically in this way it becomes clear that the familiar equations of the conical sections will all produce fractal patterns, for example the asymptote equations of the hyperbola. The ordinary hyperbola is:

$$\frac{X^2}{a^2} - \frac{Y^2}{b^2} = 1. \quad -(60)$$

Let:

$$Y = mX + c \quad -(61)$$

be an asymptote of Eq. (60). Then:

$$(a^2m^2 - b^2)X^2 + 2a^2mcX + a^2(b^2 + c^2) = 0. \quad -(62)$$

The asymptote approaches the hyperbola at infinity, so both roots of Eq. (62) are infinite:

$$a^2m^2 - b^2 = 0, \quad -2a^2mc = 0. \quad -(63)$$

The asymptotes of the ordinary hyperbola (60) are therefore:

$$Y = \pm \frac{b}{a} X. \quad -(64)$$

For the hyperbola with orbital centre at a focal point:

$$\frac{(X - a\epsilon)^2}{a^2} - \frac{Y^2}{b^2} = 1 \quad -(65)$$

and its asymptotes are:

$$Y = \pm \frac{b}{a}(X - a\epsilon) \quad -(66)$$

where:

$$X = -a\epsilon + r\cos\theta, \quad Y = r\sin\theta. \quad -(67)$$

These well known equations are transformed into fractal equations using:

$$\theta \rightarrow x\theta. \quad -(68)$$

In the centred hyperbola defined by Eq. (60) the asymptotes are the straight lines:

$$\frac{Y}{X} = \tan\theta = \pm\frac{b}{a} \quad -(69)$$

but in the fractal hyperbola:

$$\frac{Y}{X} = \tan(x\theta) = \pm\frac{b}{a} \quad -(70)$$

with an infinite array of new properties. Similarly Eq. (66) becomes the fractal asymptote:

$$\frac{Y}{X} = \tan(x\theta) = \pm\frac{b}{a} \mp \frac{b\epsilon}{X} \quad -(71)$$

where:

$$X = -a\epsilon + \frac{\alpha\cos(x\theta)}{1+\epsilon\cos(x\theta)} \quad -(72)$$

Finally, for the fractal hyperbola:

$$\frac{dY}{dX} = 2\alpha^2 \operatorname{cotan}(x\theta) \quad -(73)$$

again with completely new properties in mathematics.

It is well known that the effective potential of the H atom in the Schroedinger equation {14} is:

$$U(r) = -\frac{e^2}{4\pi\epsilon_0 r} + \frac{l(l+1)\hbar^2}{2mr^2} \quad -(74)$$

where -e is the charge on the electron, ϵ_0 the vacuum permittivity, l the orbital angular momentum quantum number, $\hbar$ the reduced Planck constant and m the electron mass. In a thought experiment, a direct comparison of Eqs (15) and (74) produces the following results:

$$k x^2 = \frac{e^2}{4\pi\epsilon_0} \quad -(75)$$

and

$$(x^2 - 1) k\alpha = \ell(\ell+1)\hbar^2 / m \quad -(76)$$

Here:

$$e = 1.60219 \times 10^{-19} \text{ C}$$
$$4\pi\epsilon_0 = 1.112650 \times 10^{-10} \text{ J}^{-1} \text{C}^2 \text{ m}^{-1}$$
$$m = \text{electron mass} = 9.10953 \times 10^{-31} \text{ kg}$$
$$M = \text{proton mass} = 1.67265 \times 10^{-27} \text{ kg}$$
$$G = 6.67265 \times 10^{-11} \text{ m}^3 \text{ s}^{-2} \text{ kg}^{-1} \quad -(77)$$

so:

$$x = 4.474467 \times 10^{19} \quad -(78)$$

for the H atom. From Eqs. (3) and (76):

$$(x^2 - 1) L^2 = \ell(\ell+1)\hbar^2 \quad -(79)$$

so to an excellent approximation:

$$L = (\ell(\ell+1))^{1/2} \frac{\hbar}{x} \quad -(80)$$

The magnitude of the angular momentum in quantum mechanics is:

$$L_0 = (\ell(\ell+1))^{1/2} \hbar \quad -(81)$$

so:

$$L = \frac{L_0}{x} \quad -(82)$$

Under the conditions (78) and (82) the two potentials (15) and (74) are the same.

The existence of a gravitational Schroedinger equation may be deduced as follows.

The original Schroedinger equation for H is:

$$\hat{H}\psi = E\psi \quad -(83)$$

where the hamiltonian operator is:

$$\hat{H} = -\frac{\hbar^2}{2m}\nabla^2 - \frac{e^2}{4\pi\epsilon_0}\cdot\frac{1}{r} \quad -(84)$$

From Eq. (75):

$$\frac{e^2}{4\pi\epsilon_0} \rightarrow mMGx^2 \quad -(85)$$

and from Eq. (76):

$$\frac{\hbar^2}{2m} \rightarrow \frac{(x^2-1)L^2}{2m\ell(\ell+1)} = \frac{(x^2-1)}{x^2}\frac{\hbar^2}{2m} \quad -(86)$$

using Eq. (82). So the gravitational Schroedinger equation is:

$$\hat{H}\psi = E\psi, \quad -(87)$$

$$\hat{H} = -\left(\frac{x^2-1}{x^2}\right)\frac{\hbar^2}{2m}\nabla^2 - x^2\frac{mMG}{r} \quad -(88)$$

Conversely the Schroedinger equation becomes an H atom fractal orbit equation of type (44) under the conditions (75), (76) and (82). The half right latitude of the H atoms' fractal orbit equation is:

$$\alpha = \frac{\ell(\ell+1)\hbar^2}{(x^2-1)m^2MG} \quad -(89)$$

where m is the electron mass and M the proton mass. So:

$$\alpha = 5.33413 \times 10^{-11}\, \ell(\ell+1). \quad -(90)$$

The eccentricity is given by:

$$\epsilon = \left(1 + \frac{2|E|\alpha}{nMG}\right)^{1/2} \quad -(91)$$

where $|E|$ is the modulus or absolute value of the energy eigenvalues of the H atom:

$$|E| = \frac{me^4}{32\pi^2\epsilon_0^2\hbar^2} \cdot \frac{1}{n^2} = \frac{2.2}{n^2} \times 10^{-18}\ J, \quad -(92).$$

where n is the principal quantum number {14}. Therefore the fractal electron orbit equation of the H atom is defined by:

$$\alpha = 5.33413 \times 10^{-11}\, \ell(\ell+1), \quad -(93)$$

$$\epsilon = \left(1 + 2.30845 \times 10^{39}\, \frac{\ell(\ell+1)}{n^2}\right)^{1/2}, \quad -(94)$$

$$x = 4.474467 \times 10^{19}, \quad -(95)$$

for each atomic orbital.

These calculations are intended as a thought experiment to illustrate the fact that the gravitational potential (15) and the effective potential (74) have the same mathematical structure.

3. GRAPHICAL PROOFS OF THE QUALITATIVE FAILURE OF EGR AND GRAPHICAL ILLUSTRATIONS OF FRACTAL CONICAL SECTIONS AND ORBITS.

ACKNOWLEDGMENTS

The British Government is thanked for a Civil List pension to MWE and the staff of AIAS and others for many interesting discussions. Dave Burleigh is thanked for posting, and Alex Hill, Robert Cheshire and Simon Clifford for translation and broadcasting. The AIAS is established in the Newlands Family Trust (2012).

REFERENCES

{1} M. W. Evans, Ed., "Definitive Refutations of Einsteinian General Relativity" (Cambridge International Science Publishing, CISP, www.cisp-publishing.com, 2012), special issue six of ref. (2).

{2} M. W. Evans, Ed., Journal of Foundations of Physics and Chemistry, (CISP, from June 2011, six issues a year).

{3} M. W. Evans, S. Crothers, H. Eckardt and K. Pendergast, "Criticisms of the Einstein Field Equation" (CISP, 2011).

{4} M. W. Evans, H. Eckardt and D. W. Lindstrom, "Generally Covariant Unified Field Theory" (Abramis Academic, 2005 to 2011) in seven volumes.

{5} L. Felker, "The Evans Equations of Unified Field Theory" (Abramis Academic, 2007, Spanish translation by Alex Hill on www.aias.us).

{6} K. Pendergast, "The Life of Myron Evans" (CISP, 2011).

{7} M. W. Evans and S. Kielich, Eds., "Modern Nonlinear Optics" (Wiley , New York, 1992, 1993, 1997, 2001), in two editions and six volumes.

{8} M .W. Evans and L. B. Crowell, "Classical and Quantum Electrodynamics and the B(3) Field" (World Scientific, 2001).

{9} M. W. Evans and J. - P. Vigier, "The Enigmatic Photon" (Kluwer, 1994 to 2002) in ten

volumes hardback and softback.

{10} M .W Evans and A. A. Hasanein, "The Photomagneton in Quantum Field Theory" (World Scientific, 1994).

{11} S. P. Carroll, "Spacetime and Geometry: an Introduction to General Relativity" (Addison Wesley, New York, 2004, and online notes 1997).

{12} R. M. Wald, "General Relativity" (Univ. Chicago Press, 1984).

{13} J. B. Marion and S. T. Thornton, "Classical Dynamics of Particles and Systems" (Harcourt Brace College Publishing, 3rd edition, 1988).

{14} P. W. Atkins, "Molecular Quantum Mechanics" (Oxford University Press, 1983, 2nd ed.)

Fractal conical sections and orbits: qualitative failure of the Einsteinian General Relativity

M. W. Evans*, H. Eckardt†, R. Delaforce and G. J. Evans
Civil List, A.I.A.S. and UPITEC

(www.webarchive.org.uk, www.aias.us,
www.atomicprecision.com, www.upitec.org)

3 Gaphical proofs of the qualitative failure of EGR and graphical illustrations of fractal conical sections and orbits

In this section we show the incorrectness of EGR by some graphical examples and evaluate some properties of fractal conical sections graphically.

3.1 Gaphical proofs of the qualitative failure of EGR

We start with a plot of the angular function $\theta(r)$ derived from Lagrange and Einstein theory. From the experimentally determined orbit (1) we obtain

$$\theta = \frac{1}{x}\ \mathrm{acos}\left(\frac{1}{\epsilon}(\frac{\alpha}{r} - 1)\right), \tag{96}$$

while Einstein theory gives

$$\theta = \frac{1}{x}\ \mathrm{acos}\left(\sqrt{1 - \frac{\alpha^4\left(\frac{1}{b^2} - \left(\frac{1}{r^2} + \frac{1}{a^2}\right)\left(1 - \frac{r0}{r}\right)\right)^2}{\epsilon^4\, x^4}}\right) \tag{97}$$

with parameters defined in (3) and (7). Using the values

$$\begin{aligned} x &= 1 \\ m &= 1 \\ M &= 100 \\ L &= 10 \\ E &= -10 \\ G &= 0.5 \\ c &= 1 \end{aligned}$$

*email: emyrone@aol.com
†email: horsteck@aol.com

gives an ellipse with $\alpha = 2, \epsilon = 0.447$. For the Lagrange theory we obtain a consistent function $\theta(r)$ with θ varying between 0 ane π, see Fig.1. For the Einstein theory, however, the square root argument is negative in the whole range so that no curve for θ comes out at all. Setting $E = 1$ leads to an elliptic orbit with $\epsilon = 1.04$. We obtain a correct function $\theta(r)$ for Lagrange theory again but a totally different cuve for Einstein theory (Fig.2).

Similar results are obtained for the derivatives $dr/d\theta$. The calculated curves from the results in Fig.2 are shown in Fig.3, in addition with the function obtained from Einstein theory directly (Eq.(6)). All three curves differ, in particular the derivatives obtained from Eq.(97) and Eq.(6) are totally different. There are severe inconsistencies in Einstein theory.

A similar effect is seen when comparing the linear velocities (13) and (14). In Fig.4 the Einstein value is graphed for three choices of the constant c. We used this constant for adopting the curve to realistic results. For higher values of c there is no solution in the whole θ range so c has to be adopted in a way that v is defined. The second curve of Fig.4 is compared to the result of Lagrange theory with $x = 1$ in Fig.5. It can be seen that both cannot be made congruent, even for other choices of c.

3.2 Graphical illustrations of fractal conical sections and orbits

The linear velocity v of Lagrange theory for several values of x is graphed in Fig.6. Although the orbits are quite different for these values, the variation of v is the same within a scaling factor on the θ axis. In this plot with cartesian coordinates this comes out quite clearly. Similar results hold for the cartesian components of the orbit itself (Figs.7-10). The X and Y component are quite quite different for elliptic, parabolic and hyperbolic orbits as expected, but varying x means a scaling of the θ axis again. The fractal nature of the orbits comes out vividly only in the polar coordinate representation.

In order to depict this, two fractal orbits are graphed in Figs.11 and 12 for x values significantly deviating from unity. For $x = 0.5$ the planet oscillates between two radii, while for $x = 0.3$ the motion between the two exremal radii is more complicated.

Finally we have plotted the orbits of two real double star systems, the Hulse-Taylor pulsar and the double neutron star J0737-3039 which has the highest precession factor x hitheto observed in astronomy. Since the latter has a low eccentricity, the deviation from a circular orbit is small. the precession of the ellipse in the Hulse-Tayler pulsar is much more evident. The radius decrease is only in the range of millimeters per revolution.

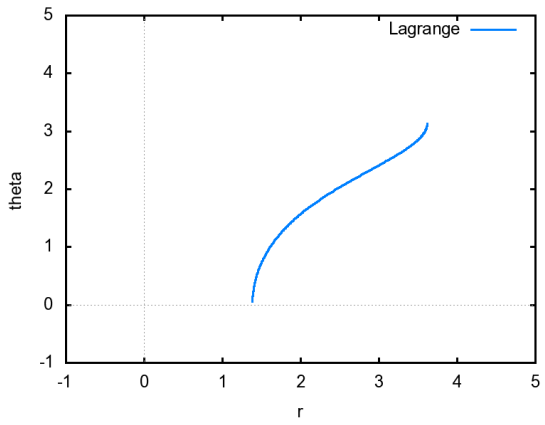

Figure 1: Angle function comparison $\theta(r)$ for an ellipse ($\alpha = 2,\ \epsilon = 0.447$).

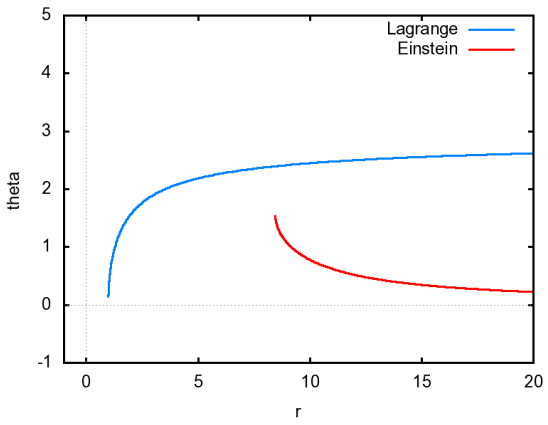

Figure 2: Angle function comparison $\theta(r)$ for a hyperbola ($\alpha = 2,\ \epsilon = 1.04$).

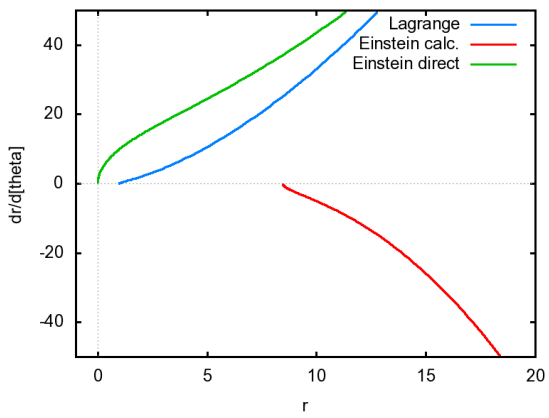

Figure 3: Comparison of derivatives $dr/d\theta$ for a hyperbola ($\alpha = 2,\ \epsilon = 1.04$).

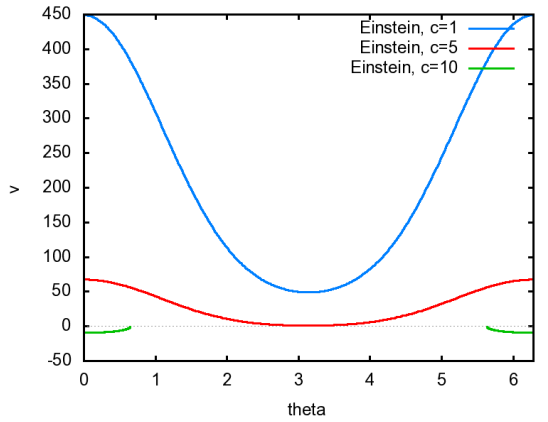

Figure 4: Linear velocity of Einstein theory for three values of c.

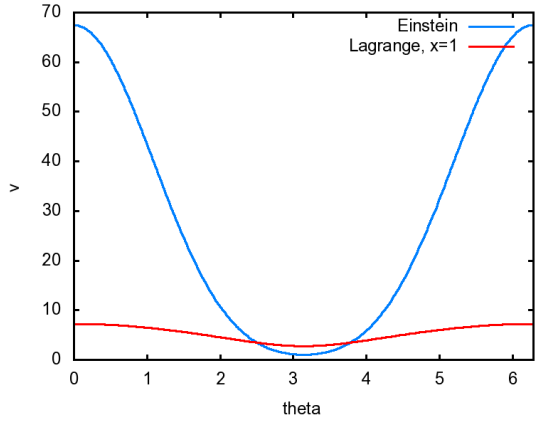

Figure 5: Comparison of Einstein and Lagrange theory.

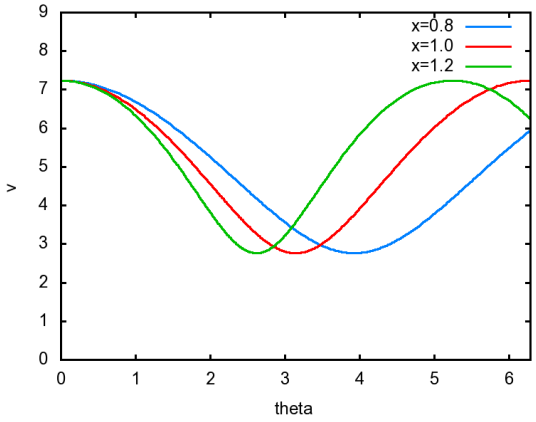

Figure 6: Linear velocity of Lagrange theory for three values of x.

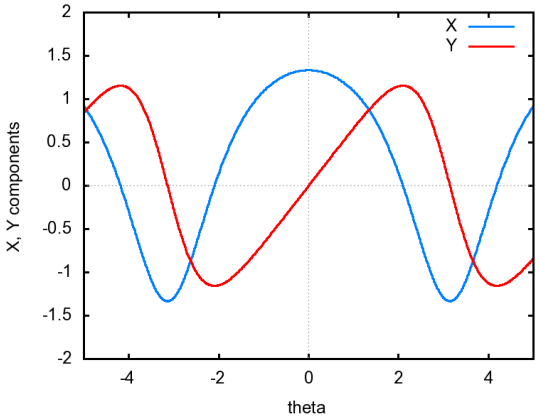

Figure 7: Cartesian X and Y components of an elliptical orbit ($\epsilon = 0.5$).

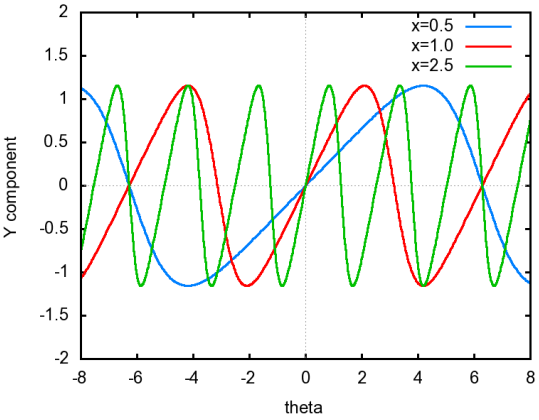

Figure 8: Cartesian Y component of an elliptical orbit for three values of x ($\epsilon = 0.5$).

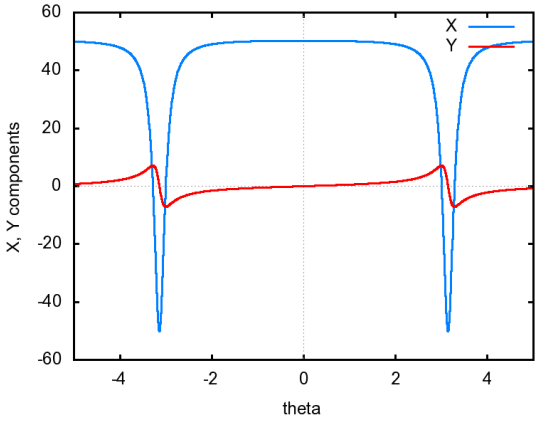

Figure 9: Cartesian X and Y components of a nealry parabolic orbit ($\epsilon = 0.99$).

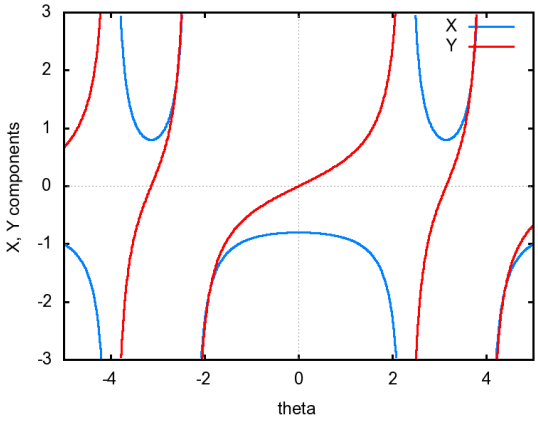

Figure 10: Cartesian X and Y components of a hyperbolic orbit ($\epsilon = 1.5$).

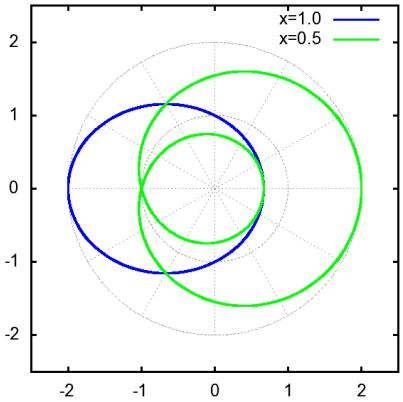

Figure 11: Stable fractal elliptical orbit for $\epsilon = 0.5$, compared to Newtonian orbit.

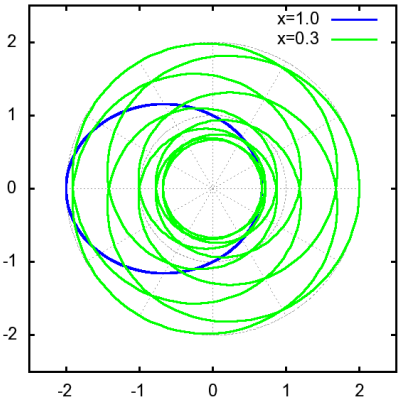

Figure 12: Unstable fractal elliptical orbit for $\epsilon = 0.5$, compared to Newtonian orbit.

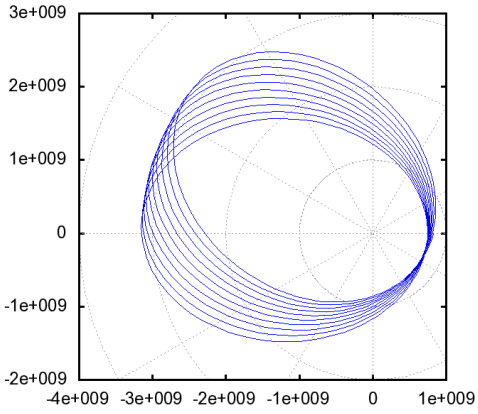

Figure 13: Orbit of the Hulse-Taylor pulsar ($\alpha = 1.207718 \cdot 10^9 m, \epsilon = 0.617131,\ x = 1.0117$).

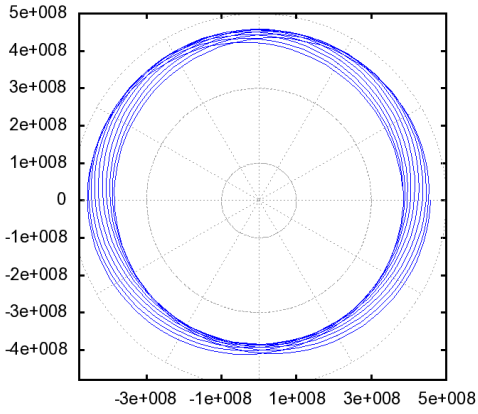

Figure 14: Orbit of the double neutron star J0737-3039 ($\alpha = 4.18 \cdot 10^8 m, \epsilon = 0.088,\ x = 1.0469$).